Texture Formation Mechanism of Vapor-Deposited fcc Thin Film on Polycrystal or Amorphous Substrate

Zhilin Li,*,†,‡ Huibin Xu,‡ and Shengkai Gong‡

College of Materials Science and Engineering, Beijing University of Chemical Technology, Beijing 100029, China and College of Materials Science and Engineering, Beijing University of Aeronautics and Astronautics, Beijing 100083, China

Received: December 31, 2003

The texture of thin films is of wide concern because it can directly affect the properties and the applications of the film. The formation mechanism of the texture should be known first in order to control the character and content of the texture. On the basis of the empirical electron theory of solid and molecules and statistical mechanics, the formation of the texture of vapor-deposited fcc thin film on polycrystal or amorphous substrate is explained with the calculation result of the valence electron structure of elements. Not only is the appearance of the (111) and (100) texture of the films convincingly explained, but the transformation order of random orientation→ (100) texture→ (100) + (111) texture→ (111) texture accompanying the rise of substrate temperature is also explained reasonably. The theory and method can also be used to explain the texture formation of films with other crystal structures.

1. Introduction

The texture in thin film has long been drawing much attention because various predominant orientations will cause the change of the film properties, which directly determine the application of the film. To control and utilize the texture effectively, the formation mechanism should be known first. As early as 1957, Kehoe[1] made a series of research studies on the heteroepitaxy of Cu, Ag, and Au of various thickness on NaCl at various temperature, but he did not give a convincing explanation of the observed texture. At first, heteroepitaxy was explained with the geometrical similarity, such as small lattice mismatching, between the film and the substrate. Because this method is simple and easy to understand, it is still used today.[2−4] But it is too coarse, so it is not in accord with some experimental results. Furthermore, when the substrate is polycrystal or amorphous, its atom arrangement is irregular, so there is no definite geometrical similarity between the film and its substrate. The growth and texture formation mechanism are still of concern today,[5,6] so they have to be explained in another way.

Now, many new test methods, such as high-resolution electron microscopy (HREM), atomic force microscopy (AFM), and scanning tunneling microscopy (STM), have been used to observe the nucleation, growth, and structure of thin films.[7−11] These methods are so powerful that the atom arrangement on the surface can be directly observed. Images of absorbed dimer were already obtained on the surface of substrates.[7,8] Homoepitaxy film growth on amorphous substrate was also observed with these methods.[9,10] However, the growth of thin films from atoms deposited from the gas phase is intrinsically a nonequilibrium phenomenon governed by a competition between kinetics and thermodynamics,[7] so the ideal research method should be real-time observation which is a very difficult task. Hannon et al. studied the real-time kinetics of a phase transformation confined to the silicon (111) surface with low-energy electron microscopy,[12] but the image they obtained of new phase with the smallest size is as large as about 100 nm. Another excellent work is the observation of the near-critical-size clusters formed during the crystallization of apoferritin.[13,14] The nucleus or absorbed cluster of film deposition is much smaller than those of apoferritin, so the real time observation of them is still a difficult task today.

With the rapid development of computers, many numerical methods are widely used to simulate the real condition in materials. Among them, ab initio simulation, molecular dynamics (MD) simulation, and Monte Carlo simulation are popular in research of the surface and interface of thin film.[9,10,15] Quantum theory is quite safe,[16,17] so ab initio simulations are convincing. But this method is only suitable for the systems with small clusters. The MD method is more effective. The classical MD method with a semiempirical potential to describe the interaction between atoms is now believed to be the only practicable method to simulate a system that consists of a few thousands or more atoms.[15] It is believed that the calculations involving millions of atoms are now feasible with the advent of massively parallel computers.[18] Now, Monte Carlo and MD methods are combined to simulate the texture competition during thin film deposition.[19,20] Those results are partially verified in titanium nitride thin films so they are helpful to elucidate the mechanisms of texture formation. However, validity of that kind of simulation result is still controlled by the reliability of the semiempirical potential. Perhaps an alternative method is needed to describe this process.

In 1962, Walton[21] gave an expression for the density of clusters of atoms using statistical mechanics and derived the nucleation rate of vapor deposition from the expression on a kinetic basis. On the basis of this formula, he deduced the existence of the (111) and (100) texture of vapor-deposited fcc films. Although Walton's model looks too coarse, it is easy to understand, so it is still a widely accepted explanation of texture.

* To whom correspondence should be addressed. E-mail: Zhlinlibj@sohu.com. Tel: +86-10-64411283. Fax: +86-10-64437587.

† Beijing University of Chemical Technology.

‡ Beijing University of Aeronautics and Astronautics.

10.1021/jp031364r CCC: $27.50
Published on Web 09/04/2004

TABLE 1: Hybridization Table of Ag

σ	1	2	3	4	5	6	7	8	9
$C_{t\sigma}$	0	0.0001	0.0002	0.0017	0.0248	0.0498	0.0585	0.2003	0.2752
$n_{T\sigma}$	5	5.0002	5.0004	5.0034	5.0496	5.0996	5.1170	5.4006	5.5504
$n_{l\sigma}$	1	1	1	1	1	1	1	1	1
$n_{c\sigma}$	4.0000	4.0002	4.0005	4.0035	4.0497	4.0995	4.1169	4.4006	4.5503
$R(1)$(nm)	0.13170	0.13170	0.13170	0.13170	0.13166	0.13163	0.13161	0.13140	0.13129
σ	10	11	12	13	14	15	16	17	18
$C_{t\sigma}$	0.3104	0.3399	0.4806	0.7887	0.8703	0.9310	0.9925	0.9958	1
$n_{T\sigma}$	5.6208	5.6797	5.9611	6.5774	6.7405	6.8621	6.9850	6.9917	7
$n_{l\sigma}$	1	1	1	1	1	1	1	1	1
$n_{c\sigma}$	4.6208	4.6797	4.9611	5.5774	5.7405	5.8621	5.9850	5.9917	6.0000
$R(1)$(nm)	0.13123	0.13119	0.13098	0.13052	0.13039	0.13030	0.13021	0.13021	0.13021

Furthermore, Walton's deduction has no relation with substrate, so a reasonable explanation of the texture on polycrystal or amorphous substrate may be developed from it. But in the further discussion to explain the texture transformation from (111) to (100) of Ag film on NaCl when substrate temperature rises, he had to consider the different effects of Cl^- and Na^+ of the substrate.[22,23] In fact, this explanation is still in the limit of heteroepitaxy, partly because Walton had to neglect the fact that the binding energy of an atom to the nucleus can be of great difference.[23]

In 1978, Yu established the empirical electron theory of solid and molecule (EET).[24−26] With the bond length difference method (BLD) in that theory, the covalent electron pair numbers of all bonds in a crystal with known lattice constant can be easily calculated so that the bond energy can also be calculated.[27] A brief introduction of EET is given in Appendix I.

Now, more and more experiment facts of the texture of fcc metal film, such as Ag, Au, Cu, Al, Ni, and Pb on polycrystal or noncrystal substrate have been accumulated.[28−32] As far as we know, all of them are of (111) or (100) predominant orientation. Among them is the most noticeable discovery of Grantscharova and Dobrev[28] based on a systemic experiment of Ag/glass film at various substrate temperatures and deposition rate. Their results show that only ⟨111⟩ is the predominant orientation when the substrate temperature is high enough or the deposition rate is low enough. With the decrease of the temperature or the increase of the deposition rate, the predominant orientation changes into the mixture of ⟨111⟩ + ⟨100⟩ and finally changes into ⟨100⟩ only. This orientation transformation order is contrary to that of epitaxial Ag film on NaCl.[22]

With EET, the various binding energy of an atom to the nucleus neglected in Walton's model can be taken into account. On this basis the texture formation mechanism of vapor-deposited fcc thin film on polycrystal or noncrystal substrate is advanced, which is in accordance with all the experiment results within our knowledge.

2. Valence Electron Structure Analysis

Take Ag as an example. In EET, dumb pair electrons, magnetic electron, covalent electron, and lattice electron are denoted by ||, ↑, ●, and Φ, respectively. When the covalent electron and lattice electron are equivalent electrons, they are denoted by •, $\underline{\Phi}$, or s′, p′, respectively. In EET, the hybridization states of Ag are given as

	d	s	p
the h state: $4d^{10}5s^1 \rightarrow 4d^8 5s^1 5p'^2$	|| || • •	Φ	• • ◦
the t state: $4d^{10}5p^1 \rightarrow 4d^7 5s'^1 5p'^3$	|| • • •	$\underline{\Phi}$	• • •

So $l = 1$, $m = 2$, $n = 2$, $\tau = 0$; $l' = 1$, $m' = 3$, $n' = 3$, $\tau' = 0$. For Ag, there is $R_h(1) = 0.13170$ nm, $R_t(1) = 0.13020$ nm. Substituting these parameters into the k formula, the hybridization table of Ag can be calculated as shown in Table 1.

For a structure with known lattice constant, the atom state of every kind of atom can be ascertained and the corresponding valence electron distribution on every bond can be calculated with the bond length difference (BLD) method in EET. The calculation process is shown in the following example.

The structure unit of Ag for bond length difference analysis is shown in Figure 1. For Ag, the lattice constant $a = 0.40862$ nm. Only three bonds of it should not be neglected which are represented by B_α (α = A, B, C). Their experiment bond lengths are as the following:

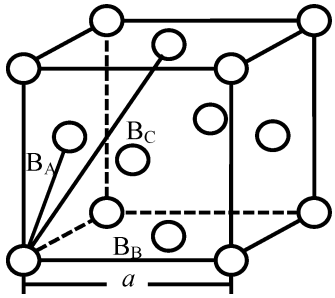

Figure 1. fcc Crystal cell and its covalent bonds.

$$D_A = \frac{\sqrt{2}}{2}a \tag{1}$$

$$D_B = a \tag{2}$$

$$D_C = \left(a^2 + \frac{1}{2}a^2\right)^{1/2} \tag{3}$$

Their equivalent bond number I_α of B_α in a structure unit of a molecule is defined as the following:

$$I_\alpha = I_M I_S I_K \tag{4}$$

where I_M represents the reference atom number in the structure or the molecule; I_S represents the equivalent bond number for a reference atom to form B_α ; I_K is a parameter that equals 1 when the two atoms that form the bond are of the same kind or 2 when the two atoms are of different kinds. For Ag, there are $I_A = 4 \times 12 \times 1 = 48$, $I_B = 4 \times 6 \times 1 = 24$ and $I_C = 4 \times 12 \times 1 = 48$, respectively.

According to the bond length formula in EET, the bond length of the B_α formed by atoms u, v should be

$$D_\alpha^{u-v} = R_u(1) + R_v(1) - \beta \lg n_\alpha \tag{5}$$

Here $\beta = 0.0600$ nm.

TABLE 2: Valence Electron Structure of Ag

$a = 0.40862$ nm	$\sigma = 8$	$R_\beta(1) = 0.13140$ nm	$n_c^8 = 4.4006$	
bond	I_α	D_α(nm)	$\bar{D}_\alpha$(nm)	n_α	ΔD_α(nm)
B_A	48	0.28894	0.28908	0.36476	0.00014
B_B	24	0.40862	0.40876	0.00369	0.00014
B_C	48	0.50046	0.50060	0.00011	0.00014
$\Sigma Ir = 48.25727$		$\Sigma n_c = 18.20131$		$\beta = 0.0600$ nm	

In our case, both the atoms u, v are Ag, therefore

$$D_\alpha = 2R(1) - \beta \lg n_\alpha \tag{6}$$

where $R(1)$ represents the single bond radii of Ag at certain hybrid level.

Take the BLD treatment

$$D_A - D_B = [2R(1) - \beta \lg n_A] - [2R(1) - \beta \lg n_B] = \beta \lg \frac{n_B}{n_A} \tag{7}$$

$$D_A - D_C = [2R(1) - \beta \lg n_A] - [2R(1) - \beta \lg n_C] = \beta \lg \frac{n_C}{n_A} \tag{8}$$

Let $r_A = 1$, $r_B = n_B/n_A$, and $r_C = n_C/n_A$, then

$$\lg r_B = \lg \frac{n_B}{n_A} = (D_A - D_B)/\beta \tag{9}$$

$$\lg r_C = \lg \frac{n_C}{n_A} = (D_A - D_C)/\beta \tag{10}$$

Substitute the bond lengths D_A, D_B, and D_C calculated with eqs 1−3 into eqs 9 and 10, the ratios $r_B = n_B/n_A$ and $r_C = n_C/n_A$ can be calculated.

A structure unit should be electron neutral, so the covalent electron of all the j atoms in the unit should be distributed on all the α (= A, B, C.....) covalent bonds in it. In other words, the total covalent electron number of all the j atoms $\sum_j n_{cj}$ should equal the sum of the electron number on all the covalent bonds in the unit $\sum_\alpha I_\alpha n_\alpha$; i.e.

$$\sum_j n_{cj} = \sum_\alpha I_\alpha n_\alpha = \sum_\alpha n_A I_\alpha r_\alpha = n_A \sum_\alpha I_\alpha r_\alpha \tag{11}$$

$$n_A = \frac{\sum_j n_{cj}}{\sum_\alpha I_\alpha r_\alpha} = \frac{4n_c}{48r_A + 24r_B + 48r_C} \tag{12}$$

For certain hybrid level σ of Ag, the covalent electron number n_c^σ and bond radii $R_\sigma(1)$ can be found in the hybridization table (Table 1), so the covalent electron distribution on the bonds, i.e., n_A, n_B, n_C can be calculated. For the 18 hybrid levels of Ag, there should be 18 groups of distribution. So the hybrid states of the atoms and the corresponding distributions which are in accordance with the actuality have to be determined.

In EET, the bond lengths calculated with the calculated n_α are called theoretical bond lengths which are represented by $\bar{D}_\alpha$. Substituting the calculated n_α into eq 5, there should be

$$\bar{D}_\alpha = R_u(1) + R_v(1) - \beta \lg n_\alpha = 2R_\sigma(1) - \beta \lg n_\alpha \tag{13}$$

Bond length difference (BLD) ΔD_α, is the absolute value of the difference between the experimental bond length and the theoretical one, i.e.:

$$\Delta D_\alpha = |D_\alpha - \bar{D}_\alpha| \tag{14}$$

In EET, $\Delta D_\alpha < 0.005$ nm is the criterion to determine whether the given atom state and the corresponding valence electron distribution accord with reality. If $\Delta D_\alpha < 0.005$ nm, they are considered to be in accordance with reality. The atom states and the corresponding electron distribution are called the valence electron structure (VES) of the solid or molecule in EET.

In this case, the parameters of the 18 hybrid levels of Ag in Table 1 are substituted into the related formulas to calculate 18 groups of n_α and 18 groups of ΔD_α. For Ag, there are 12 groups of BLD which satisfy $\Delta D_\alpha < 0.005$ nm. Among them we take the hybrid level with the smallest ΔD_α and the corresponding covalent electron distribution as the VES of Ag which is shown in Table 2.

Table 2 shows that there are 0.36476 covalent bond pairs on the strongest bond B_A of Ag. But on B_B and B_C, there are only 0.00369 and 0.00011 covalent bond pairs, respectively. So they are much weaker bonds than B_A. It is the obvious difference of these bonds that effects the formation of the texture of vapor-deposited Ag film.

3. Analysis of the Formation of the Texture in Vapor Deposition Process

3.1 Walton's Theory. In the vapor deposition process, the critical nucleus is very small. As early as 1954, Yang and his colleagues concluded from their experiment that it contains only 9 atoms.[33] For such small clusters almost all atoms are on the surface, so the concept of macroscopic surface energy is no longer valid. In this case, the nucleation process should not be treated with methods for larger clusters, such as the spherical-drop model.

To solve this problem, Walton calculated the concentration of clusters with statistical mechanics.[21] He supposed that when an atom forms part of a cluster its potential energy is decreased and the value of the decrease is equal to its binding energy in the cluster. With this assumption he calculated the density nucleation rate of some possible two-dimensional adsorbed clusters with given size and structure which are shown in Figure 2. He also deduced the size and structure of the critical nucleus

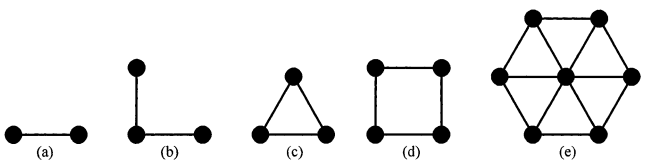

Figure 2. Structure of clusters in Walton's assumption.

at various temperatures. In general, he derived that the nucleation rate of two- or three-dimensional small nuclei has the following form:

$$I = R\frac{\sigma_n}{a}\left(\frac{Ra^2}{\nu}\right)^n \exp\left[(nQ_{ad} + Q_{ad} + E_{n^*} - Q_D)\frac{1}{kT}\right] \quad (15)$$

where I represents the nucleation rate; R is the rate of incidence of atoms from the vapor; a is the separation between adsorption sites; n is the number of atoms of the cluster; σ_n is the capture width of the critical nucleus for a single atom so that the resulting configuration will be a stable cluster; ν is an attempt frequency; Q_{ad} is the additional energy of an atom to form a three-dimensional nucleus; E_{n^*} is the binding energy of the cluster which is related to the size n and the structure of the cluster; Q_D is the activation energy for surface diffusion; k is Boltzmann constant; and T is the substrate temperature.

According to eq 15, various clusters have different parameters, such as E_{n^*}, so they are stable at various temperatures. Walton deduced that the higher the substrate temperature is, the larger the stable cluster should be. So when the substrate temperature is low, the stable nucleus has the structure of Figure 2a, the second atom can combine with the first atom (the critical nucleus) in a random way, so the cluster would not possess a single direction. When the temperature rises, the critical nucleus has two atoms and takes the structure of Figure 2a. The third atom is added to the critical nucleus to form the stable nucleus with the structure of Figure 2c. With this "building block" for the deposit, the deposit should be oriented with a (111) plane parallel to the substrate. If the substrate temperature rises higher, the stable nucleus would take the structure of Figure 2d. This building block would lead to a (100) plane parallel to the substrate.

Walton's theory successfully gives an explanation of the (100) and (111) textures of fcc films. However, according to his explanation, the (100) texture should appear at a higher substrate temperature than that of (111) texture, which is opposite to Grantscharova's experimental result.[28] The experiment has been repeated at various substrate temperatures and incidences, so there must be mistakes in Walton's theory. In fact, our calculation result has shown that the bonds of the films are of various numbers of covalent electron pairs, which is different from Walton's assumption that all bonds are of the same bond energy. Considering this fact, the texture of the film can be explained more convincingly.

3.2 Analysis of the Formation of the Texture. Our calculation has already shown that B_A, B_B, and B_C have various covalent electron pair numbers, so the bond energies of these bonds are not the same. Because all atoms in this case are of the same kind, the bond energy of the bond is only determined by its bond length. In Walton's model only bond B_A is considered. But B_B and B_C should not be neglected. For example, it is unreasonable that there is no bond between the atoms at the two ends of the cluster of Figure 2b. In fact there should be a B_B bond between them. Consider B_B: Figure 2b with three atoms also has the delta shape like Figure 2c, the only difference is that their bonds are of different bond length and bond energy. A similar case occurs in Figure 2d. Taking B_B and B_C into account, the clusters that have relation to the formation of the texture can be shown in Figure 3.

With this consideration, the following analysis can be advanced.

When the substrate temperature is low, the critical nucleus has only one atom. The second atom is absorbed to form a stable nucleus which has the structure of Figure 3a. With this building block the film has no preferential orientation. This case has already been described in Walton's model.

When the substrate temperature is higher, the critical nucleus has two atoms with the structure of Figure 3a. The third atom

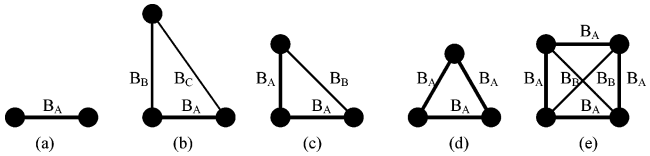

Figure 3. Structure of clusters related to the formation of the texture.

is absorbed to form a stable nucleus. However, the third atom has various possible ways to combine with the first two, which have no difference in Walton's model. When it forms one B_B and one B_C, the cluster has the structure of Figure 3b which can be considered to be the building block of the (110) plane of fcc crystals. When it forms one B_A and one B_B, the cluster has the structure of Figure 3c which can be considered to be the building block of the (100) crystal plane. When it forms two B_A, the cluster has the structure of Figure 3d which can be considered to be the building block of the (111) crystal plane.

In Walton's opinion,[21] when an atom forms part of a cluster, its potential energy decreases by a constant value equal to its binding energy in the cluster. Walton also gives the concentration of cluster with n atoms[21]

$$N_n/N_0 = (N_1/N_0)^n \exp(E_n/kT) \quad (16)$$

where N_0 is the number of adsorption sites; and N_1 is the number of clusters with only one atom. Assume that the larger the number of covalent electron pairs a bond has, the larger binding energy it has. When a cluster respectively takes the structure of Figure 3b, c, d, its total number of covalent electron pairs is $n_A + n_B + n_C = 0.36476 + 0.00369 + 0.00011 = 0.36856$, $2n_A + n_B = 2 \times 0.36476 + 0.00369 = 0.73321$, and $3n_A = 3 \times 0.36476 = 1.09428$, respectively. So the concentration of the cluster with the structure of Figure 3b is the smallest because of its smallest E_n.

Furthermore, in Figure 3b, the third atom connects with the first two through one B_B and one B_C bond; on them there are only $n_B + n_C = 0.00369 + 0.00011 = 0.00380$ covalent electron pairs which is much smaller than that on a single B_A, i.e. $n_A = 0.36476$. So this kind of connection is very weak. The third atom is bonded with the first two even weaker than it is on the line of the first two. Therefore this cluster is not as stable as that having the structure of Figure 3a. Being the most unstable cluster and with the smallest concentration, this kind of nucleus is supposed to have a very small possibility to exist. Now that the building block of (110) crystal plane probably does not exist, it is natural that (110) texture has not been discovered in so many experiments so far.

As for Figure 3c and d, the third atom connected with the first two through $B_A + B_B$ and two B_A, respectively. The total covalent electron pair number of them are $n_A + n_B = 0.36476 + 0.00369 = 0.36845$, $2n_A = 2 \times 0.36476 = 0.72952$, respectively. Obviously both of them are larger than $n_A = 0.36476$, so both of these kinds of clusters can be stable nuclei which exist at the higher substrate temperature than that of Figure 3a. Although both of them are possible two-dimensional nuclei, the nucleus of Figure 3d is stable at higher substrate temperature than that of Figure 3c because of its larger binding energy. In the middle temperature, they can exist simultaneously. Up to now, the existence of the (100) and (111) texture in vapor-deposited films and their transformation order of (100)→ (100) + (111)→(111) has already been explained.

When the substrate temperature becomes still higher, the critical nucleus becomes three atoms or more, so the stable nucleus has four or more atoms. Such a nucleus can be three-

TABLE 3: Main Valence Electron Structure Parameters of Some fcc Metals

element	a (nm)	σ	n_A	n_B	n_C	ΔD_α(nm)
Cu	0.36150	A9	0.37568	0.00646	0.00029	0.00048
Au	0.40786	9	0.37715	0.00385	0.00011	0.00007
Ni	0.35238	A13	0.52554	0.01001	0.00048	0.00124
Al	0.40494	4	0.20834	0.00510	0.00027	0.00003

dimensional which will not be the building block of any single crystal plane, so it will not cause any preferential orientation. Therefore at the substrate temperature above the existence of (111) texture, the texture probably disappears. According to Walton's calculation, for a large fraction of the possible experiment conditions the nucleation rate drops off so rapidly that when a minimum of three bonds per atom (which means the nucleus has at least four atoms) is required for a stable cluster, the nucleation rate is already very small.[21] For example, when the incidence rate R is one monolayer per second, the nucleation rate I of a five-atom cluster is less than 1 cm^{-2} s^{-1} at its stable temperature. So the texture disappearance at higher temperature is rarely reported. The only evidence we found is Hashimoto and his colleague's experiment result[30] which shows that Ni film on the glass of 213 K has (111) texture, whereas that on the glass of 333 K has no texture. The deposition rate of the experiment is 5 nm s^{-1}. The lattice constant of Ni is a = 0.35238 nm, so its (111) interplanar distance is $\sqrt{3}\ a/4$ = 0.15259 nm. Therefore the deposition rate is 5/0.15259 = 32.8 layers per second. At so large a value of R, it is reasonable that the nucleation rate I of the nucleus with over four atoms is large enough to cause the disappearance of the (111) texture.

Another noticeable fact is that the nucleus with four or more atoms can also be plane such as those of Figure 2e and Figure 3e. The former has seven atoms, so its nucleation rate I is very low under the common experiment conditions according to Walton's calculation.[21] Even if it does appear, it can also be the building block of (111) plane and will cause no new texture. As for Figure 3e, it can be a building block of (100) plane, so it may cause (100) texture at the temperature above (111) texture. However, its nucleation rate is much smaller than that of the nucleus shown in Figure 3d. Furthermore, every atom of the Figure 3e nucleus has two B_A and one B_B; the total number of covalent electron pairs is only $2n_A + n_B = 2 \times 0.36476 + 0.00369 = 0.73321$ which is only a little larger than that of Figure 3d of $2n_A = 2 \times 0.36476 = 0.72952$. So even if the nucleus of Figure 3e does exist, it will be difficult to separate it from that of Figure 3d. This analysis accords well with the experimental result of Adamik and colleagues[31] that the (111) texture of Ag thin film on amorphous quartz substrates is always accompanied by a weak (100) texture. As far as we know, no independent (100) texture has been reported above the temperature of (111) texture.

The valence electron structures of other fcc metals, such as Cu, Au, Ni, and Al, are also calculated, and their main VES parameters are listed in Table 3. These metals also have various n_A, n_B, n_C, and their strength orders are the same as that of Ag. Therefore all above analysis is suitable for them. Now it can be considered that the regulation can be expanded to all fcc metals.

4. Summary

The stability of clusters in the vapor was deduced with the valence electron pair numbers on their bonds as calculated with EET. The nucleation rate I of clusters was considered with Walton's theory. On these bases, the competition between kinetics and thermodynamics was considered. So the formation of the texture of fcc films on polycrystal or amorphous substrate in vapor deposition process can be explained reasonably. The explanation is not only concerned with the substrate temperature and the deposition rate, but is also in good accordance with experimental results. So this kind of method can also be expanded to other structures such as bcc and hcp metals. Furthermore, because the analysis does not require the films to be of a single element, it may also be expanded to compounds and solid solutions whose valence electron structure can also be calculated with EET. The first expansion on bcc metal will be published in another paper.

Acknowledgment. This work was emphatically supported by the Science and Technology Foundation of the Chinese Ministry of Education (Grant 02018) and the China Postdoctoral Science Foundation.

Appendix I: A Brief Introduction of the Empirical Electron Theory of Solid and Molecules (EET)

The foundation of EET is based on an inductive method. It took over 30 years from the beginning of its theoretical research to publish. During those years, Prof. Yu had analyzed and summarized energy band theory, covalent bond theory, and Hume−Rothery's electron concentration theory systematically. Meanwhile, a number of modern experiment results (such as neutron scattering, electron diffraction, microwave, Mossbauer effect, spin resonance, positron annihilation, and Compton scattering), 78 elements in the periodic table of the first six periods (except for rare gases elements), thousands of crystalline and molecular structures, alloy phase diagrams, and a series of data on physical properties had been put together to check and systemize EET. Under the first-order approximation, the calculated and analyzed results of EET agree with experimental data. Since the publication of EET, many Chinese researchers have been engaged in its theoretical research and application with great interest. So far, more than 10 branches have been formed. These fields include mechancs, thermodynamics (such as melting point, boiling point, coefficient of linear expansion, cohesive energy of elements, alloys and compounds, thermal conductivity), electromagnetics (including electron conductivity, magnetic moment, high temperature superconductivity, etc.), binary alloys phase diagrams and phase transitions, high compression phase transitions, and so on. The main points of EET are briefly introduced in the following.

EET is based on L. Pauling's electron theory of metals and quantum theory. The general conclusions drawn from the investigation are summarized in four hypotheses.

Hypothesis I. In general, the atomic state in solids and molecules is a hybridization of two atomic states, which are called the h (head) and t (tail) states. At least one of them is the ground or near excited state. Both of them correspond to two stationary states, and a certain atomic state is the overlap of the two states. Both the h and t states have their own number of covalent electrons n_c, lattice electron n_l, and the single bond radius $R(1)$, which was first introduced by Pauling. To understand this hypothesis, the introduced terms and their experimental foundations are as follows:

1. For the atomic state, the hybridization is similar to that of the traditional concept, i.e., two Russell−Saunders structures are coupled based on L. Pauling's theory. But there is a little difference: the atomic states in EET may be described by magnetic, covalent, and lattice electrons. The experimental foundations of their existence are as follows: (a) The electronic distribution curves of CoAl and NiAl prove the existence of a

covalent bond in alloys according to Cooper's report. (b) The lattice electron comes from an s electron. When the s energy band is wide, the electron might reach an energy level above the Fermi energy. The electron can hover in a space of 3−5 atoms, even in that of more than 6 atoms. Hence, the movement of electrons can be regarded as in lattice spaces under a periodic field, which are distributed in the lattice space freely, and more or less without the necessity to form an electronic pair having spin just opposite of each other. The earliest support of this recognition came from the nonrelativistic and relativistic band structure of Pb in the formation of the $6s^2$ band. The electronic equidensity curves of Cu, Ag, and NiAl are direct evidence of the existence of lattice electrons.

2. The introduction of $R(1)$ is based on the reason that hybridization can change the distance between the peak position of charge density of the atomic orbit and atomic nucleus. The value of $R(1)$ corresponds to the covalent radius.

3. The valence number of the covalent bond is derived from a report of Home-Rothery and L. Pauling.

Hypothesis II. Hybridizations of the states are quantized and the relative compositions C_h for the h state and C_t for the t state are given by

$$C_t = \frac{1}{1+k^2}, \quad C_t + C_h = 1 \tag{A1}$$

$$k = \frac{\tau' l' + m' + n'}{\tau l + m + n} \cdot \sqrt{\frac{l' + m' + n'}{l + m + n}} \cdot \frac{l \pm \sqrt{3m} \pm \sqrt{5n}}{l' \pm \sqrt{3m'} \pm \sqrt{5n'}} \tag{A2}$$

where l, m, n and l', m', n' represent the sum of the numbers of s, p, d covalent electron and lattice electron of the h and t state, respectively. The terms τ and τ' are parameters for the h and t states, respectively, and value 1 when the s electron is covalent electron or 0 when the s electron is lattice electron. The terms $k = \infty$ and $k = 0$ represent the h and t states, respectively. The number of various k values is called hybrid level number.

In the case of $\tau = m = n = 0$, equation (A2) is substituted by the following form:

$$k = \sqrt{\frac{l' + m' + n'}{l}} \cdot \frac{l' + m' + n'}{l' \pm \sqrt{3m'} \pm \sqrt{5n'}} \tag{A3}$$

The character parameters describing the atomic state at σ hybrid level can be given with the following formulas:

$$n_{l\sigma} = n_{lh}C_{h\sigma} + n_{lt}C_{t\sigma} = (1-\tau)lC_{h\sigma} + (1-\tau')l'C_{t\sigma} \tag{A4}$$

$$n_{c\sigma} = n_{ch}C_{h\sigma} + n_{ct}C_{t\sigma} = (\tau l + m + n)C_{h\sigma} + (\tau' l' + m' + n')C_{t\sigma} \tag{A5}$$

$$R(1)_\sigma = R(1)_h C_{h\sigma} + R(1)_t C_{t\sigma} \tag{A6}$$

Hypothesis III. Except in some special conditions, there will always be covalent electron pairs between two adjacent atoms u and v. The number of this covalent electron pair is represented by n_α, and the distance between these two atoms is called covalent bond length, which is represented by D_α^{uv} here. According to Pauling's equation

$$D_\alpha^{uv} = R_u(1) + R_v(1) - \beta \lg n_\alpha (\text{nm}) \tag{A7}$$

Where u and v may or not be the same kind of atoms, n_α can be an integer or a fraction, α = A, B, C$\cdots$N represents all bonds that cannot be neglected in a structure. Here a modification for Pauling's original theory is made as the following:

$$\beta = \begin{cases} 0.0710 \text{ nm} & \text{when } n_\alpha^M < 0.25 \quad \text{or } n_\alpha^M > 0.75 \\ 0.0600 \text{ nm} & \text{when } 0.300 \le n_\alpha^M \le 0.700 \\ 0.0710 - 0.22\epsilon \text{ (nm)} & \text{when } n_\alpha^M = 0.250 + \epsilon \quad \text{or } n_\alpha^M = 0.750 - \epsilon \end{cases} \tag{A8}$$

where $0 \le \epsilon < 0.050$, n_α^M represents the largest n_α in the structure.

Hypothesis IV. For B groups of elements, including the transition metals Ga, In, and Tl, a portion of d electrons on the outside layer of their atoms expands so far that their influence on covalent bond length equals the effect of the s or p electrons on the utmost outside layer. For Cu, Ag, and Au, the distributions of their p valence electrons in various cells in the lattice space are so chaotic that their average effect equals that of s electrons. However, the phase angle distribution of these equivalent electrons and their contribution to cohesive energy still keeps the original characters. Equivalents are represented by ●, Φ, or s′, p′.

Appendix II: Hybridization States in EET of the Elements

1 A type and A_1 type of Ni

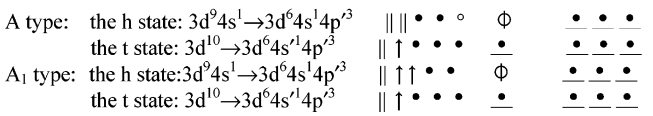

$l = 1$, $m = 3$, $n = 2$, $\tau = 0$; $l' = 1$, $m' = 3$, $n' = 3$, $\tau' = 1$
$R_h(1) = 0.11950$ nm, $R_t(1) = 0.11379$ nm

2 B type of Ni

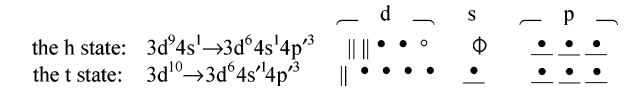

$l = 1$, $m = 3$, $n = 2$, $\tau = 0$; $l' = 1$, $m' = 3$, $n' = 4$, $\tau' = 1$
$R_h(1) = 0.11950$ nm, $R_t(1) = 0.10950$ nm

3 A type of Cu, Ag, and Au

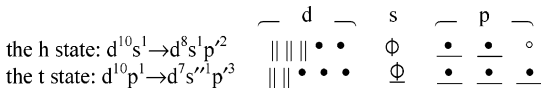

$l = 1$, $m = 2$, $n = 2$, $\tau = 0$; $l' = 1$, $m' = 3$, $n' = 3$, $\tau' = 0$
Cu: $R_h(1) = 0.11520$ nm, $R\ (1) = 0.11380$ nm
Ag: $R_h(1) = 0.13170$ nm, $R\ (1) = 0.13020$ nm
Au: $R_h(1) = 0.13190$ nm, $R_t(1) = 0.13030$ nm

4 B type of Cu

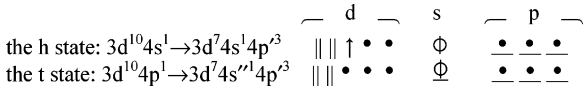

$l = 1$, $m = 3$, $n = 2$, $\tau = 0$; $l' = 1$, $m' = 3$, $n' = 3$, $\tau' = 0$
$R_h(1) = 0.11853$ nm, $R_t(1) = 0.11380$ nm

5 A type of Al

$l = 2$, $m = 1$, $n = 0$, $\tau = 0$; $l' = 1$, $m' = 2$, $n' = 0$, $\tau' = 1$
$R_h(1) = 0.11900$ nm, $R_t(1) = 0.11900$ nm

References and Notes

(1) Kehoe, R. B. *Philos. Mag.* **1957**, *2*, 455.
(2) Shi, Z.; Craib, G. R. G.; Playe, M. A.; Tang, C. C. *Thin Solid Films* **1997**, *304*, 170.
(3) Jiang, X.; Schiffmann, K.; Klages, C.-P. *J. Appl. Phys.* **1998**, *83*, 2511.
(4) Wang, L.; Liu, X.; Zan, Y.; Wang, J.; Wang, D.; Lu, D.; Wang, Z. *Appl. Phys. Lett.* **1998**, *72*, 109.
(5) Paulmier, D.; Huu, T. L.; Zaidi, H. *Surf. Sci.* **1997**, *866*, 377.
(6) Bartholmei, S.; Fouquet, P.; Witte, G. *Surf. Sci.* **2001**, *473*, 227.
(7) Zhang, Z.; Lagally, G. M. *Science* **1997**, *276*, 377.
(8) Qin, X. R., Lagally, M. G. *Science* **1997**, *278*, 1444.
(9) Furman, I.; Biham, O.; Zuo, J.; Swan, A. K.; Wendelken, J. F. *Phys. Rev.* **2000**, *B62*, R10649.
(10) Pauwels, B.; Tendeloo, G. V.; Bouwen, W.; Kuhn, L. T.; Lievens, P.; Lei, H.; Hou, M. *Phys. Rev.* **2000**, *B62*, R10383.
(11) Everitt L. D., Miller J. W. W., Abbott, N. L.; Zhu, X. D. *Phys. Rev.* **2000**, *B62*, R4833.
(12) Hannon, J. B.; Hibino, H.; Bartelt, N. C.; Swartzentruber, B. S.; Ogino, T.; Kellogg, G. L. *Nature* **2000**, *405*, 552.
(13) Yau, S.-T.; Vekilov, P. G. *Nature* **2000**, *406*, 494.
(14) Oxtoby, D. W. *Nature* **2000**, *406*, 464.
(15) Hou, Q.; Hou, M.; Bardotti, L.; Prevel, B.; Melinon, P.; Perez, A. *Phys. Rev.* **2000**, *B62*, 2835.
(16) Friedman, J. R.; Patel, V.; Chen, W.; Tolpygo, S. K.; Lukens, J. E. *Nature* **2000**, *406*, 43.
(17) Blatter, G. *Nature* **2000**, *406*, 25.
(18) Zhou, S. J.; Preston, D. L.; Lomeahl, P. S.; Beaziey, D. M. *Science* **1998**, *279*, 1525.
(19) Huang, H.; Gilmer, G. H.; Diaz de la Rubia, T. *J. Appl. Phys.* **1998**, *84*, 3636.
(20) Huang, H.; Gilmer, G. H. *J. Comput.-Aided Mater. Des.* **2001**, *7*, 203.
(21) Walton, D. *J. Chem. Phys.* **1962**, *37*, 2182.
(22) Walton, D. *Philos. Mag.* **1962**, *7*, 1671.
(23) Walton, D.; Rhodin, T. N.; Rollins, R. W. *J. Chem. Phys.* **1963**, *38*, 2698.
(24) Yu, R. *Chin. Sci. Bull.* **1978**, *23*, 217 (in Chinese).
(25) Guo, Y.; Yu, R.; Zhang, R.; Zhang, X.; Tao, K. *J. Phys. Chem.* **1998**, *B102*, 9.
(26) Liu, Z.; Li, Z.; Sun, Z. *Metall. Mater. Trans.* **1999**, *30A*, 2757.
(27) Zhang, R. *Empirical Electron Theory in Solid and Molecule*; Jilin Science and Technology Publishing House: Changchun, China, 1990; pp 268−287 (in Chinese).
(28) Grantscharova, E. *Thin Solid Films* **1993**, *224*, 28.
(29) Narayana, G. S.; Misra, N. K. *Thin Solid Films* **1988**, *164*, 91.
(30) Hashimoto, T.; Okamoto, K.; Fujiwara, H.; Itoh, K.; Kamiya, M.; Hara, K. *Thin Solid Films* **1991**, *205*, 146.
(31) Adamik, M.; Barna, P. B.; Tomov, I. *Thin Solid Films* **2000**, *359*, 33.
(32) Tomov, I.; Adamik, M.; Barna, P. B. *Thin Solid Films* **2000**, *371*, 17.
(33) Yang, L.; Birchenall, C. E.; Pound, G. M.; Simnad, M. T. *Acta Metall.* **1954**, *2*, 462.